

## INFLUENCE OF MECHANICAL ACTIVATION AND HEAT TREATMENT ON MAGNETIC PROPERTIES OF NANOSTRUCTURED MIXTURE



M. M. Vasić<sup>a</sup>, A. S. Kalezić-Glišović<sup>b</sup>, R. Milinčić<sup>c</sup>, Lj. Radović<sup>d</sup>,  
D. M. Minić<sup>d</sup>, A. M. Maričić<sup>b</sup>, D.M. Minić<sup>a\*</sup>

<sup>a</sup> Faculty of Physical Chemistry, University of Belgrade, Belgrade, Serbia

<sup>b</sup> Faculty of Technical Sciences, University of Kragujevac, Čačak, Serbia

<sup>c</sup> Kapiolani Community College, University of Hawaii System, USA

<sup>d</sup> Military Technical Institute, Belgrade, Serbia

(Received 09 August 2018; accepted 03 January 2019)

### Abstract

The mechanical activation of the  $\text{Ni}_{85.8}\text{Fe}_{10.6}\text{Cu}_{2.2}\text{W}_{1.4}$  powder mixture in the time intervals of 30–210 min in combination with thermal treatment at 393–873 K resulted in microstructural changes, forming the nanostructured mixture of the same composition but improved magnetic properties. The best result were achieved for mechanical activation during 120 min and thermal treatment at temperatures close to the Curie temperature (693K), enhancing the mass magnetization of the starting powder mixture by about 57%. The microstructural changes, which include the structural relaxation, decrease in free volume, density of dislocation and microstrain, improve structural characteristics of material, enabling better mobility of walls of magnetic domains and their better orientation in applied magnetic field and consequently enabling better mass magnetization of the material. With longer time of milling, the growing stress introduced in the sample undergoes easier relief, relocating stress-relieving processes toward lower temperatures.

**Keywords:** Nanostructured mixture; Mechanical activation; Annealing; Structural relaxation; Mass magnetization; Enthalpy.

### 1. Introduction

Nanocrystalline powders are single-phase or multi-phase materials with the crystal size of the order of a few (typically 1–100) nanometers in at least one dimension. Because of the extremely small size of the grains, a large fraction of the atoms in these materials is located in the grain boundaries resulting in favorable combination of physical, mechanical and magnetic properties. Generally speaking, sintered nanocrystalline powders show increased strength, high hardness, extremely high diffusion rates, and consequently reduced sintering times for powder compaction [1]. The technical progress and development of new technologies has been significantly accelerated with the development of new amorphous, as well as nanostructured metals or their alloys. These materials have found application in different areas due to their specific electrical, magnetic, mechanical, anti-corrosion and other properties [2 - 7].

It was shown that nickel/iron alloys have good mechanical, electrical, and magnetic properties and a

high catalytic activity for some electrochemical reactions [8–10]. Enrichment of these alloys with small quantities of tungsten improves their thermal stability as well as their wear resistance, corrosion resistance, microhardness, and prevents thermal oxidation [11–20]. NiFeW alloys may exhibit the crucial properties of NiW and FeW alloys without the unwanted properties of the two-component alloys. They are widely used in industries, mainly as inductor cores for electromagnets [21–23], magnetic devices [24], microwave noise filters [25], magnetic recording heads [26] and tunable noise suppressors [27]. The metallurgical fabrication of these nanostructured alloys is expensive due to tungsten's high melting point. Therefore, other procedures for their production have been recommended, such as mechanical alloying, sputtering, or electrolytic deposition from water baths [11–18, 28–30]. Well-sized nanocrystals are supposed to be obtained by adding a small portion of Cu to the initial alloy composition [31].

During the last couple of decades, a number of new materials have been obtained by means of a powder sintering. One of the most important

\*Corresponding author: [dminic@ffh.bg.ac.rs](mailto:dminic@ffh.bg.ac.rs)



techniques used as a starting procedure for obtaining nanostructured materials by sintering is mechanochemical activation. With the proper choice of technological parameters for the mechanochemical activation process and the process of compounding and sintering of activated powders, materials of desired composition with various physical properties can be obtained [32 - 37].

A group of nanostructured powders with good ferromagnetic characteristics takes a special place in modern electronics [38]. Due to their metastable structure, these powders require special handling and study of their structural transformations induced by heating in different environments. This paper deals with the defining of optimal parameters for powder synthesis of nanostructured NiFeCuW in terms of magnetic properties.

## 2. Experimental

The initial powder was a mechanical mixture of polycrystalline powders with following weight fractions: 85.8% Ni, 10.6% Fe, 2.2% Cu and 1.4%W. Commercial metal powders were used for this purpose, without any pretreatment. The powder mixture was activated in a planetary mill within time intervals of 30, 60, 120, 150, 180 and 210 min, at 400 rpm speed, in an argon atmosphere. XRD analysis was performed to determine the average crystallite size, microstrain and minimum density of dislocations of the crystalline phases present in the activated powders. For this purpose, measurements were carried out by a Philips PW-1710 automated diffractometer, using a Cu tube operated at 40 kV and 30 mA. For data processing and identification of individual crystalline phases present in the powder mixture, PDF-2 database [39], namely cards No. 04-0850; 99-0064; 99-0034; 01-1204, and MAUD software [40] were employed.

DSC and DTA methods were used to test the thermal stability of the powder in the temperature interval from room temperature up to 1293 K, in a stream of nitrogen with a flow rate of 50 ml/min. DTA measurements were conducted on a SDT Q600 (TA instruments) at 10 K/min, while for the DSC measurements, a DSC Q1000 (TA Instruments) and a heating rate of 5 K/min were employed. The surface morphology of the initial powder mixture, as well as mechanically and thermally treated samples, was studied by means of a scanning electron microscopy (SEM), on a SEM JEOL JSM-6610LV microscope, equipped with an energy dispersive X-ray spectrometer. Magnetization of the samples obtained by pressing of the activated powders has been measured by modified Faraday balance technique [41] in the temperature interval 293-873 K at a heating rate 10 K/min, in an argon atmosphere. The applied magnetic field intensity at the place where the sample was positioned was 40 kA/m, whereas the field gradient was  $dH/dz = 4 \cdot 10^{-9}$  A/m/m.

## 3. Results and discussion

### 3.1. Microstructural changes induced by mechanical activation

The microstructural changes of the initial mixture of polycrystalline powders of Ni (85.8 wt.%), Fe (10.6 wt.%), Cu (2.2 wt.%) and W (1.4 wt.%) were studied after mechanical activation in an argon atmosphere. For this purpose, the aliquots of the powder mixture have been taken in defined time intervals (30-210 min) and analyzed by XRD (Fig. 1) and SEM technique (Figs 6-9).

The qualitative analysis of the diffractograms shows the presence of all starting crystalline components in the treated mixture, as indicated in Fig 1b. The broadening of all peaks, as well as the changes in their intensities provoked by mechanical treatment,

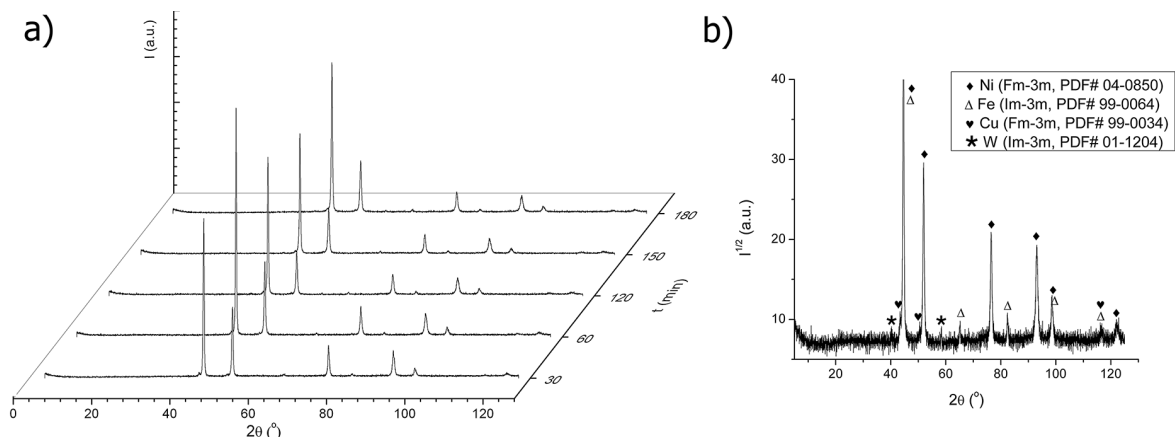


**Figure 1.** XRD diffractograms of NiFeWCu powder mixture mechanically activated for 30, 60 120, 150 and 180 min in an argon atmosphere (a); diffractogram of the sample mechanically treated for 120 min with identification of crystalline phases (b).

suggests the changes of microstructural characteristics, including crystallite size, microstrain and minimum dislocation densities for all components.

Average crystallite size,  $d$ , and microstrain values were determined by Williamson-Hall method [42], while the relation  $\rho = 3/d^2$  [43] was used to get minimum dislocation densities,  $\rho$ . Texture coefficients were determined according to the reference [44]. The calculated microstructural parameters for the two abundant crystalline phases, fcc-Ni and bcc-Fe, are supplied in Table 1.

Generally speaking, the activation of the starting mixture by milling induced a decrease in crystallite size and an increase in microstrain and minimum dislocation densities for the two chosen metal components as shown in Table 1. The rate of change in the crystallite size is a function of treatment time. For the nickel phase, at the beginning, the change in the average crystallite size occurs fast reaching the plateau and then the average crystallite size drops again, reaching the maximal rate of change at about 120-150 min of mechanical treatment, Fig. 2a. The decrease rate of average crystallite size at the beginning is  $0.43 \text{ nm min}^{-1}$  and  $0.48 \text{ nm min}^{-1}$  in the final stage. For the iron phase, the highest change in crystallite size occurs in the first 30 minutes of mechanical treatment with the rate of  $0.87 \text{ nm min}^{-1}$ . The change in microstrain occurs mostly in the first 60 minutes for the nickel phase, and in the first and last 30 minutes for the iron phase, Table 1.

The change of texture coefficient with duration of treatment, followed on the fcc-Ni phase as the abundant one, on planes (111), (200), (220) and (311), Fig. 2b, did not show any preferential orientation. This means that there is no preferential direction for crushing of the crystallites.

### 3.2. Heat treatment

Thermal stability of the untreated powder, as well as mechanically treated samples, was studied by

thermal analysis methods, DTA and DSC, in the temperature range 298-1293 K, Fig. 3. The obtained data were correlated with microstructural transformations obtained from XRD measurements.

Thermal DTA and DSC curves of the starting powder possessing certain amounts of trapped energy, Fig. 3a, 3b, exhibit only one exothermic thermal event

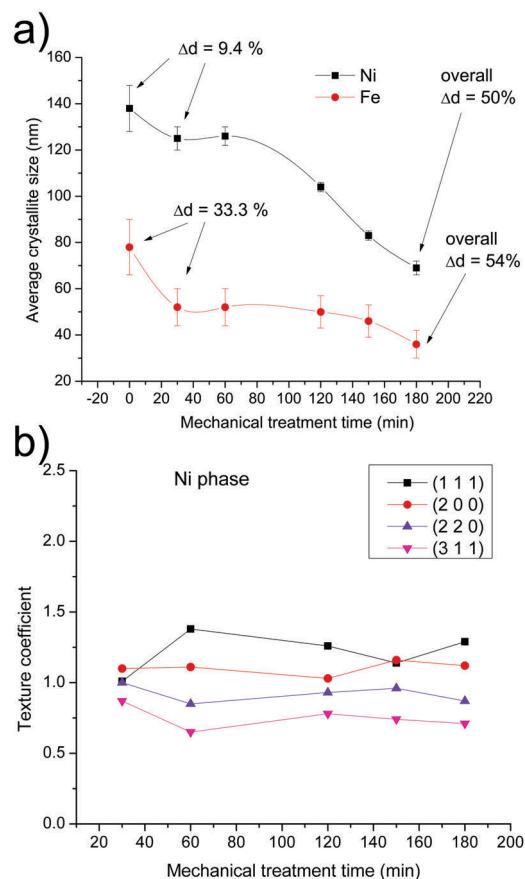


**Figure 2.** The changes of crystallite size of fcc-Ni and bcc-Fe phases (a); texture coefficient of fcc-Ni (b) as a function of duration of mechanical activation.

**Table 1.** Microstructural parameters of fcc-Ni ( $Fm\bar{3}m$ ) and bcc-Fe ( $Im\bar{3}m$ ) crystalline phases.

Milling time (min)	fcc-Ni phase			bcc-Fe phase		
	Average crystallite size (nm)	Microstrain	Minimal dislocation density ( $\text{m}^{-2}$ )	Average crystallite size (nm)	Microstrain	Minimal dislocation density ( $\text{m}^{-2}$ )
0	$138 \pm 10$	$0.0024 \pm 0.0005$	$(1.6 \pm 0.3) \cdot 10^{14}$	$78 \pm 12$	$0.0015 \pm 0.0004$	$(4.9 \pm 1.5) \cdot 10^{14}$
30	$125 \pm 5$	$0.0028 \pm 0.0003$	$(1.9 \pm 0.2) \cdot 10^{14}$	$52 \pm 8$	$0.0022 \pm 0.0007$	$(1.1 \pm 0.2) \cdot 10^{15}$
60	$126 \pm 4$	$0.0035 \pm 0.0003$	$(1.9 \pm 0.2) \cdot 10^{14}$	$52 \pm 8$	$0.0022 \pm 0.0007$	$(1.1 \pm 0.2) \cdot 10^{15}$
120	$104 \pm 2$	$0.0038 \pm 0.0003$	$(2.8 \pm 0.1) \cdot 10^{14}$	$50 \pm 7$	$0.0023 \pm 0.0007$	$(1.2 \pm 0.2) \cdot 10^{15}$
150	$83 \pm 2$	$0.0038 \pm 0.0003$	$(4.4 \pm 0.2) \cdot 10^{14}$	$46 \pm 7$	$0.0026 \pm 0.0008$	$(1.4 \pm 0.2) \cdot 10^{15}$
180	$69 \pm 3$	$0.0038 \pm 0.0003$	$(6.3 \pm 0.5) \cdot 10^{14}$	$36 \pm 6$	$0.0032 \pm 0.0009$	$(2.3 \pm 0.4) \cdot 10^{15}$
Untreated mixture heated up to 1293K	$145 \pm 20$	$0.0019 \pm 0.0007$	$(1.4 \pm 0.4) \cdot 10^{14}$	-	-	-



in the region of stress-relieving processes, in the temperature range 470-620 K [45]. During the mechanical treatment, the additional amount of stress accumulated in all treated components, affects the exothermic thermal event in the temperature range 470-620 K, Fig.3c. Well defined exo-maximum of the starting mixture undergoes broadening and compounding with prolonging the milling time, Fig 3c. The growing stress introduced in the sample with longer time of treatment undergoes easier relief, relocating the stress-relieving processes into the region of lower temperatures, with a tendency of growth of realised enthalpy, Table 2. The compounded shape of DSC peaks for prolonged time of milling indicates step-wise process of deterioration of the structure. The individual steps were characterised by peak temperatures  $T^I_{peak}$ ,  $T^{II}_{peak}$ ,  $T^{III}_{peak}$ . In order to find the peak temperature for each step of the process of deterioration of the structure, the deconvolution was performed, as presented in supplement (Fig. S2). Almost constant enthalpy value after 60 min of mechanical treatment, despite growing level of applied energy during mechanical treatment, indicates that only certain amount of energy stays trapped in the deformed structure being realised during thermally induced structural relaxation. Nevertheless, the rest of the applied energy is spent mostly on crushing of the crystallites and growth of interface region [46].

XRD of the starting powder, after DTA (up to 1293 K), indicates only slightly higher crystallite size, resulting from the thermal treatment, and somewhat lower value of microstrain and dislocation density, as observed from the study of Ni-phase, Table 1 (Fig. S1, Supplement).

**Table 2.** Enthalpy values of stress-relieving processes and DSC peak positions corresponding to different milling times;  $T^I_{peak}$ ,  $T^{II}_{peak}$ ,  $T^{III}_{peak}$  denote peak temperatures of individual steps obtained after peak deconvolution.

Milling time (min)	$T^I_{peak}$ (K)	$T^{II}_{peak}$ (K)	$T^{III}_{peak}$ (K)	Total enthalpy (J/g)
0	557	-	-	2.5
30	552	-	-	2.6
60	551.6	-	-	8.8
120	544.2	-	-	8.4
150	543.2	567	-	8.9
180	528.4	553	571.8	8.4

### 3.3 Thermomagnetic properties

Taking into consideration the effect of mechanical treatment on microstructure, as well as the influence of thermal treatment on stress-relieving processes, the functional properties significant for practical application of these materials require the study of their magnetic properties before and after thermal treatment, for prolonged time of powder milling. For these purposes, the powder of  $Ni_{85.8}Fe_{10.6}Cu_{2.2}W_{1.4}$ , before and after milling, was pressed (by applying the pressure of 500MPa) into disc-shaped pellets, 8 mm in diameter and around 1 mm in width.

As found, the magnetization of the starting powder, measured in 40 kA/m field was 23.5 Am<sup>2</sup>/kg and the Curie temperature 770K, Fig 4a. The value of Curie temperature of the starting powder, being somewhat higher than Curie temperature of nickel and

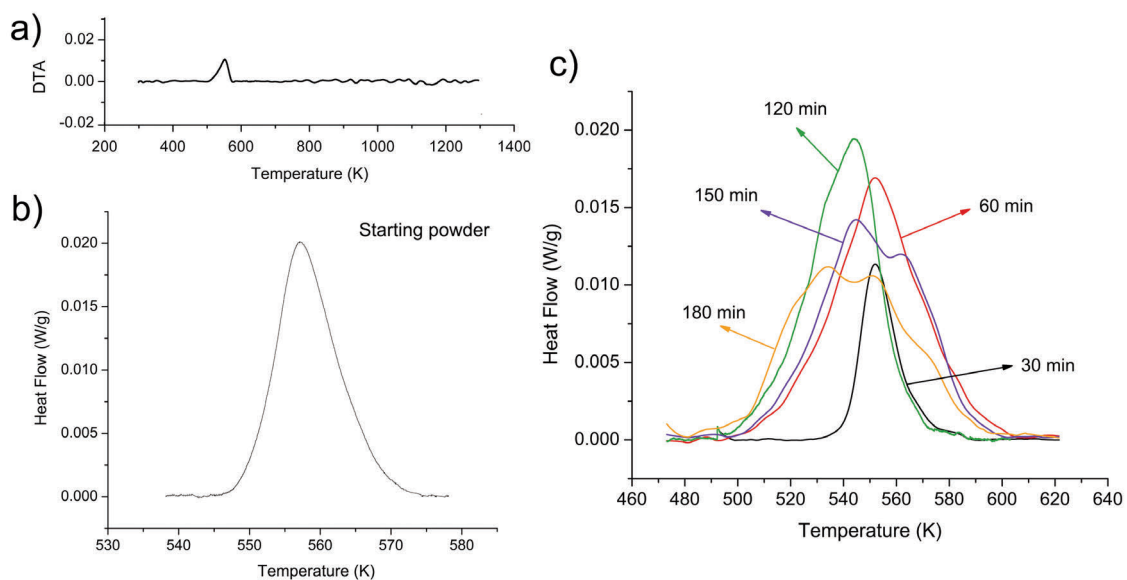


**Figure 3.** Thermal analysis in nitrogen atmosphere: DTA curve of the starting powder mixture, 10 K/min (a); DSC curve of the starting powder mixture, 5 K/min (b); DSC curves of the powders mechanically treated for 30-180 min, 5 K/min.



lower than Curie temperature of iron, is a result of the presence of both metals in the powder. Because of the stress relieving effects in the temperature range up to 500K, thermal treatment led to an increase in the magnetization of the powder which then dropped sharply approaching to the Curie temperature. The observed microstructural changes, induced by mechanical activation of the powder, influence the value of Curie temperature, which drops gradually, because of the approaching to the nickel and then iron Curie temperature.

The influence of milling duration on mass magnetization (measured in 40 kA/m field), Fig 4b, shows an increase, with the maximal value at 120 min milling. Prolonged milling leads to a decrease of mass magnetization as a result of further crushing and agglomeration of the particles accompanied by degradation of magnetic ordering [47]. For that reason, the powder mechanically treated for 120 min was chosen for further research.

Isothermal treatment of all mechanically treated powders for 10 min at 693 K, before the

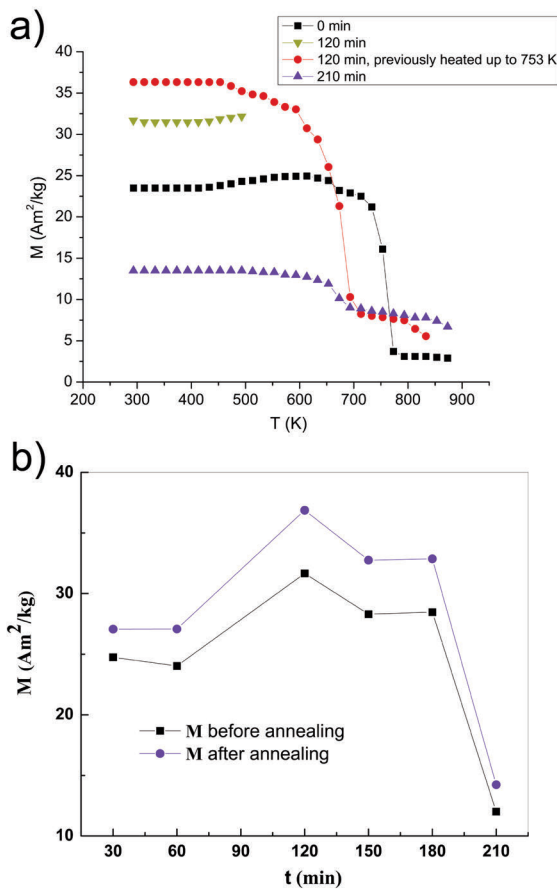


Figure 4. Mass magnetization of pressed starting and mechanically treated powders as a function of temperature (a); mass magnetization of the powder mechanically treated for different times before and after annealing at 693K for 10 min (b).

measurements of magnetization at room temperature, shows the same trend of changes of mass magnetization, but with increased mass magnetization by 14.5% on average, Fig.4b. Maximal values of mass magnetization, for mechanical activation of 120 min, were 31.7  $\text{Am}^2/\text{kg}$  before annealing and 36.9  $\text{Am}^2/\text{kg}$  after annealing of the powder.

For better understanding of the influence of annealing on magnetic properties of the studied mixture, the measurements of mass magnetization were performed during successive heating of 120 min milled powder, increasing final temperature from 393 up to temperature of 873 K, Fig. 5a. The values of magnetization for thermally treated powder, after cooling to room temperature under the magnetic field, as a function of the final annealing temperature are presented in Fig.5b.

The stress-relieving processes of thermally treated

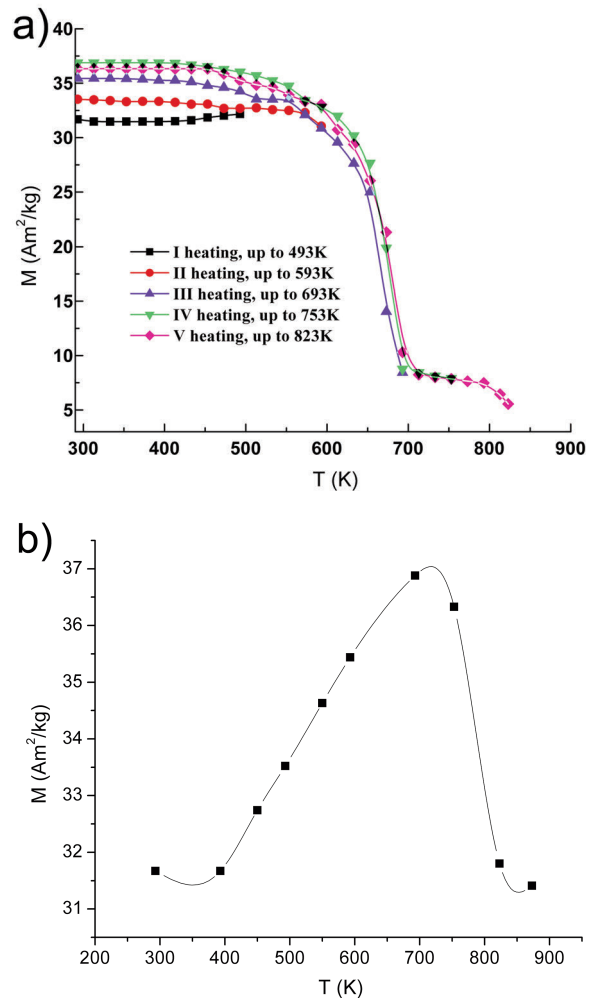


Figure 5. Temperature dependence of mass magnetization of pressed powder mechanically treated for 120 min: during successive heating (a); at room temperature as a function of the final heating temperature (b).



milled powder during the first heating cause an increase in mass magnetization of 16.4%, Fig.5a. The maximum in mass magnetization is reached by thermal treatment up to 693 K, Fig.5b, therefore this temperature is chosen for isothermal annealing, Fig 4b.

Mechanically activated pressed powder contains high fraction of free volume, high density of dislocations chaotically distributed and high level of microstrain, enabling relatively low value of mass magnetization of material annealed in the temperature region 293-393K, which precedes the region of structural relaxation. With the successive increase of annealing temperature (400-693K), provoked microstructural changes led to an increase in mass magnetization reaching the value of  $36.9 \text{ Am}^2/\text{kg}$  at 693K. The microstructural changes, which included the structural relaxation, decrease in free volume, density of dislocation and microstrain, improved structural characteristics of material, enabling better mobility of walls of magnetic domains and their better direction in applied magnetic field and consequently enabling better mass magnetization of the material. All this together led to an improvement in mass magnetization by 57% in total, 35% by mechanical activation of the powder during 120 min and 22% by annealing at temperature of 693K.

The annealing of the material at higher temperatures (753-873K) strengthens the structure

through the grain growth and coalescence, diminishes the mobility of magnetic domains walls and omits their direction in applied magnetic field and consequently diminishes the mass magnetization of the material [48].

### 3.4. Particle morphology

Changes in the particle morphology of the powder provoked by mechanical and thermal treatments were examined by SEM (secondary electron as well as back scattered electron imaging), before and after examination of the functional properties, Figs 6-9.

Crystalline particles 1-15  $\mu\text{m}$  in size can be observed in the SEM images of the powders before and after milling for different times, Fig. 6. Milled non-heated powders exhibit quite rough particle surface, similar to that of the starting, non-treated powder, with the tendency to form agglomerates of small and crushed particles, Fig. 6. SEM images did not show any significant changes in morphology of rough particles mechanically treated for 120 min with the increase of temperature, in the temperature range of observed structural relaxation and decrease of magnetic moment, Fig 7.

Different milling time in the case of pressed thermally treated samples leads to some differences in the size and packing of agglomerated polycrystalline particles, including larger agglomerates and better

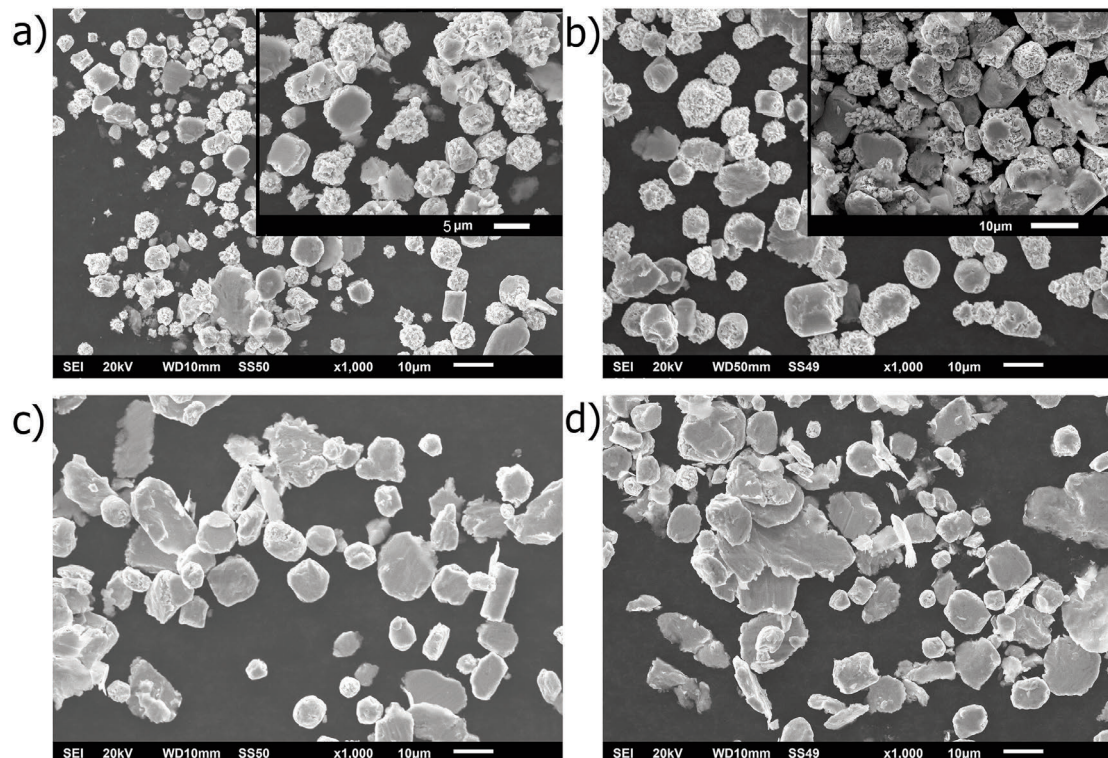


**Figure 6.** SEM secondary electron images of NiFeWCu powder mixture: untreated (a) and mechanically treated for 30 min (b), 120 min (c) and 150 min (d) (magnification 1000x). Insets represent higher-magnification images (2000-3000x).

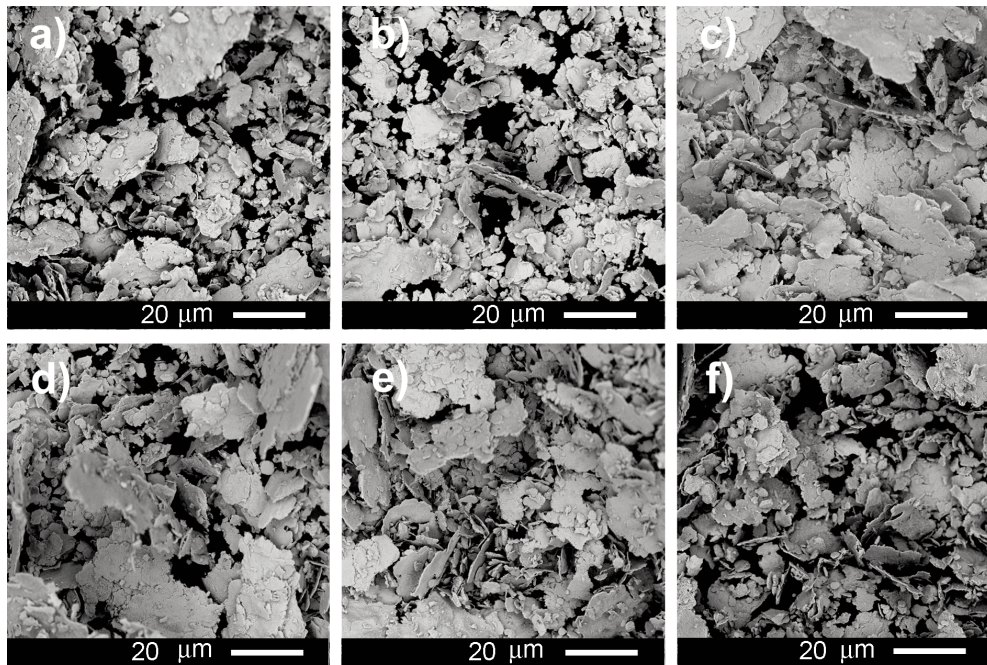


**Figure 7.** SEM back scattered electron images of NiFeWCu powder mixture mechanically treated for 120 min: non-heated (a) and heated at different temperatures: 393 K (b), 573 K (c), 693 K (d), 773 K (e), 873 K (f); (magnification 3000x).

packing with fewer hollows for longer milling times, Fig. 8. The effect similar to this was observed for the samples heated up to different temperatures (up to 693

and 873 K, 60 min milled), where thermal treatment up to higher temperature causes more coalescence, Fig. 9.

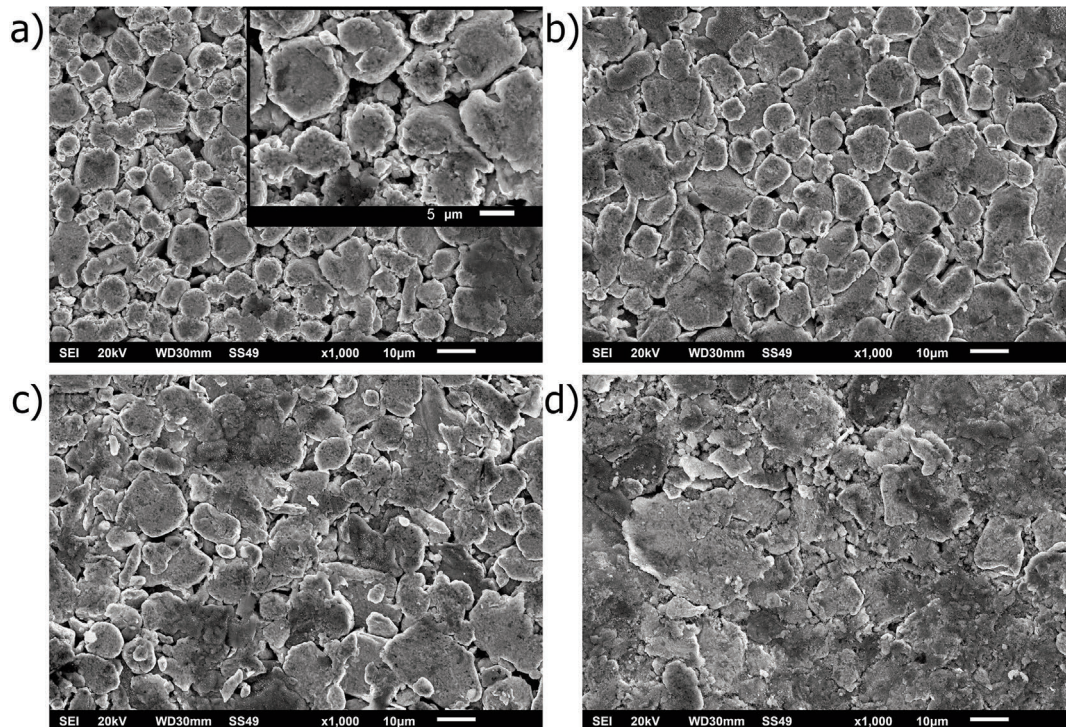


**Figure 8.** SEM secondary electron images of pressed and thermally treated (up to 873K) NiFeWCu powder mixture, mechanically treated for 30 (a), 120 (b), 150 (c) and 210 (d) min (magnification 1000x; figure in inset: magnification 3000x).

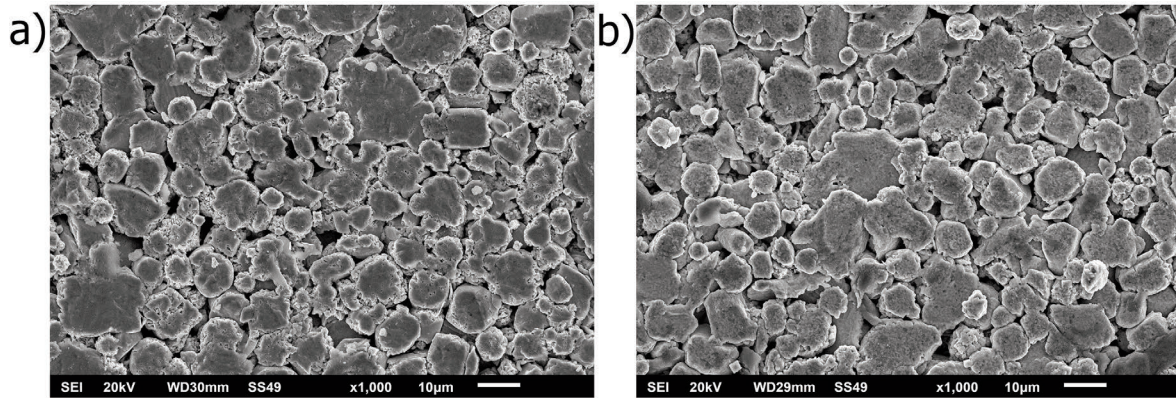


**Figure 9.** SEM secondary electron images of pressed NiFeWCu powder mixture milled for 60 min, thermally treated up to 693 K (a) and 873 K (b) (magnification 1000x).

#### 4. Conclusion

Mechanical activation of the polycrystalline powder mixture  $\text{Ni}_{85.8}\text{Fe}_{10.6}\text{Cu}_{2.2}\text{W}_{1.4}$  for different times (30-210 min) caused microstructural changes influencing its magnetic properties, and exceeding the magnetic properties of the electrodeposited NiFeW alloys of similar composition produced at a current density higher than  $50 \text{ mA cm}^{-2}$  [14]. The compounded shape of stress-relieving DSC peak for the prolonged milling suggests a step-wise process of deterioration of the structure. It was shown that mechanical activation of the powder (30-120 min), in combination with thermal treatment at temperatures close to the Curie temperature, led to the improvement in mass magnetization by about 57%, relative to the starting powder. This is a consequence of convenient coupling of microstructural changes and the stress relieving processes in the temperature region up to 600 K, which most likely resulted in easier mobility of magnetic domain walls and their orientation in magnetic field. However, high temperature annealing (>753 K) and prolonged mechanical activation of the material (> 120 min) diminish the mobility of magnetic domains walls because of the strengthening of the structure through the grain growth and coalescence, resulting in the lowering of mass magnetization of the material.

#### Acknowledgements

*This research was supported by the Ministry of Education, Science and Technological Development of the Republic of Serbia, under the Projects No. OI172015 and OI172057. The authors would like to thank Prof. Slavko Mentus (Faculty of Physical Chemistry, University of Belgrade) for recording SEM back scattered electron images.*

#### References:

- [1] C. Suryanarayana, Prog. Mater. Sci., 46 (2001) 1-184.
- [2] T. Dastagir, W. Xu, S. Sinha, H. Wu, Y. Cao, H. Yu, App. Phys. Lett., 97 (2010) Article ID 162506.
- [3] T.O. Donnell, N. Wang, S. Kulkarni, R. Meere, F.M.F. Rhen, S. Roy, S.C.O. Mathuna, J. Magn. Magn. Mater., 322 (2010) 1690–1693.
- [4] M. Vroubel, Y. Zhuang, B. Rejaei, J. Burghartz, J. Magn. Magn. Mater., 258-259 (2003) 167-169.
- [5] C. Cheung, F. Djuanda, U. Erb, G. Palumbo, Nanostructured Materials, 5 (1995) 513-523.
- [6] A. Kawashima, H. Habazaki, K. Hashimoto, Mat. Sci. Eng. A, 304-306 (2001) 753-757.
- [7] V.L. Tellkamp, E.J. Lavernia, A. Melmed, Metall. Mater. Trans. A, 32 (2001) 2335-2343.
- [8] L.X. Phua, N.N. Phuoc, C.K. Ong, J. Alloy. Compd., 520 (2012) 132–139.
- [9] M.A.O. Tolentino, E.M.A. Estrada, C.A.C. Escobedo, A.M.B. Miro, F.S.D. Jesus, R.G.G. Huerta, A.M. Robledo, J. Alloy. Compd., 536 (2012) 245–249.
- [10] K.R. Sriraman, S.G.S. Raman, S. K. Seshadri, Mater. Sci. Eng. A, 460-461 (2007) 39–45.
- [11] K.R. Sriraman, S.G.S. Raman, S.K. Seshadri, Mater. Sci. Techn., 22 (2006) 14–22.
- [12] A.O. Ijaduola, J.R. Thompson, A. Goyal, C.L.H. Thieme, K. Marken, Physica C, 403 (2004) 163-171.
- [13] M.H. Allahyarzadeh, M. Aliofkhaeaei, A.R. Rezvanian, V. Torabinejad, A.R.S. Rouhaghdam, Surf. Coat. Techn., 307A (2016) 978-1010.
- [14] M. Spasojević, N. Ćirović, L.R. Zelenović, P. Spasojević, A. Maričić, J. Electrochem. Soc., 161 (2014) D463-D469.
- [15] P. Esther, C.J. Kennady, P. Saravanan, T. Venkatachalam, Journal of Non-Oxide Glasses, 1 (2009) 301-309.
- [16] F. He, J. Yang, T. Lei, C. Gu, Appl. Surf. Sci., 253 (2007) 7591-7598.
- [17] M. Donten, H. Cesiulis, Z. Stojek, Electrochim. Acta, 45 (2000) 3389–3396.
- [18] S.J. Mun, M. Kim, T.H. Yim, J.H. Lee, T. Kang, J. Electrochem. Soc., 157 (2010) D177–D180.





- [19] N. Ćirović, P. Spasojević, L.R. Zelenović, P. Mašković, M. Spasojević, *Sci. Sinter.*, 47 (2015) 347–365.
- [20] M. Banerjee, A. Singh, A.K. Majumdar, A.K. Nigam, *J. Phys.-Condens. Mat.*, 23 (2011) Article ID 306004.
- [21] T. Dastagir, W. Xu, S. Sinha, H. Wu, Y. Cao, H. Yu, *Appl. Phys. Lett.*, 97 (2010) Article ID 162506.
- [22] E. Kubo, N. Ooi, H. Aoki, D. Watanabe, J.H. Jeong, C. Kimura, T. Sugino, *Jpn. J. Appl. Phys.*, 49 (2010) Article ID 04DB17.
- [23] T.O. Donnell, N. Wang, S. Kulkarni, R. Meere, F.M.F. Rhen, S. Roy, S.C.O Mathuna, *J. Magn. Magn. Mater.*, 322 (2010) 1690–1693.
- [24] O. Song, C.A. Ballentine, R.C.O Handley, *Appl. Phys. Lett.*, 64 (1994) 2593–2595.
- [25] C. Jiang, D. Xue, W. Sui, *Thin Solid Films*, 519 (2011) 2527–2530.
- [26] B. Koo, B. Yoo, *Surf. Coat. Tech.*, 205 (2010) 740-744.
- [27] B.K. Kuanr, R. Marson, S.R. Mishra, A.V. Kuanr, R.E. Camley, Z.J. Celinski, *J. Appl. Phys.*, 105 (2009) Article ID 07A520.
- [28] S.H. Hong, H.J. Ryu, *Mat. Sci. Eng. A*, 344 (2003) 253-260.
- [29] Z.W. Zhang, J.E. Zhou, S.Q. Xi, G. Ran, P.L. Li, W.X. Zhang, *J. Alloy. Compd.*, 370 (2004) 186-191.
- [30] Z.W. Zhang, J.E. Zhou, S.Q. Xi, G. Ran, P.L. Li, *Mat. Sci. Eng. A*, 379 (2004) 148-153.
- [31] J.S. Blázquez, V. Franco, A. Conde, *J. Phys. Condens. Matter.*, 14 (2002) 11717-11727.
- [32] S.J. Mun, M. Kim, T.H. Yim, J.H. Lee, T. Kang, *J. Electrochem. Soc.*, 157 (2010) D177–180.
- [33] R. Orrù, R. Licheri, A.M. Locci, A. Cincotti, G. Cao, *Mat. Sci. Eng. R*, 63 (2009) 127-287.
- [34] G. Herzer, *IEEE T. Magn.*, 25 (1989) 3327-3329.
- [35] E. Ivanov, C. Suryanarayana, *J. Mater. Synth. Proces.*, 8 (2000) 235-244.
- [36] A. Castro, P. Millán, L. Pardo, B. Jiménez, 9 (1999) 1313-1317.
- [37] W.S. Jung, H.S. Park, Y.J. Kang, D.H. Yoon, *Ceram. Int.* 36 (2010) 371-374.
- [38] J. Vernières, J.F. Bobo, D. Prost, F. Issac, F. Boust, *J. Appl. Phys.* 109 (2011) Article ID 07A323.
- [39] JCPDS PDF-2 Database, ICDD, Newton Square, PA, USA, 2005.
- [40] L. Lutterotti, *Nucl. Instrum. Methods B*, 268 (2010) 334-340.
- [41] S. Reutzel, D.M. Herlach, *Adv. Eng. Mater.* 3 (2001) 65-67.
- [42] G.K. Williamson, W.H. Hall, *Acta Metall.*, 1 (1953) 22–31.
- [43] G.K. Williamson, R.E. Smallman, *Philos. Mag.* 1 (1956) 34-46.
- [44] G.B. Harris, *Philos. Mag.* 43 (1952) 113-123.
- [45] A.M. Maričić, D.M. Minić, V.A. Blagojević, A.K. Glišović, D.M. Minić, *Intermetallics*, 21 (2012) 45-49.
- [46] A.S. Kurlov, A.I. Gusev, *Tech. Phys. Lett.* 33 (2007) 828-832.
- [47] G.F. Zhou, H. Bakker, *Mater. Trans. JIM* 36 (1995) 329-340.
- [48] N. Ćirović, P. Spasojević, L. Ribić-Zelenović, P. Mašković, A. Maričić, M. Spasojević, *Sci. Sinter.* 48 (2016) 1-16.

## UTICAJ MEHANIČKE AKTIVACIJE I TERMIČKE OBRADNE NA MAGNETNE OSOBINE NANOSTRUKTURNE SMEŠE $Ni_{85.8}Fe_{10.6}Cu_{2.2}W_{1.4}$

M. M. Vasić<sup>a</sup>, A. S. Kalezić-Glišović<sup>b</sup>, R. Milinčić<sup>c</sup>, Lj. Radović<sup>d</sup>,  
D. M. Minić<sup>d</sup>, A. M. Maričić<sup>b</sup>, D.M. Minić<sup>a\*</sup>

<sup>a</sup>Fakultet za fizičku hemiju, Univerzitet u Beogradu, Beograd, Srbija

<sup>b</sup>Fakultet tehničkih nauka u Čačku, Univerzitet u Kragujevcu, Čačak, Srbija

<sup>c</sup>Kapiolani koledž, Univerzitet na Havajima, SAD

<sup>d</sup>Vojnotehnički institut, Beograd, Srbija

### Apstrakt

Mehanička aktivacija  $Ni_{85.8}Fe_{10.6}Cu_{2.2}W_{1.4}$  praškaste smeše, u vremenskim intervalima od 30-210 min, u kombinaciji sa termičkom obradom na temperaturama u rasponu od 393-873 K, dovela je do mikro strukturnih promena, stvarajući nanostrukturnu smešu istog sastva, ali sa poboljšanim magnetnim osobinama. Najbolji rezultat je ostvaren za mehaničku aktivaciju u trajanju od 120 min, prilikom termičke obrade na temperaturama oko Kirijeve tačke (693K), kada je specifična magnetizacija početne smeše povećana za 57%. Mikrostrukturne promene, koje obuhvataju strukturnu relaksaciju, smanjenje slobodne zapremine, gustine dislokacije i mikronaprezanja, dovode do poboljšanja strukturnih osobina materijala, i na taj način omogućuju bolju pokretljivost zidova magnetnih domena, kao i njihovo usmeravanje u primenjenom magnetnom polju, samim tim doprinose boljoj specifičnoj magnetizaciji materijala. Sa dužim mlevenjem, veći stres akumuliran u uzorku podložniji je oslobađanju, pri čemu se procesi oslobađanja stresa pomeraju ka nižim temperaturama.

**Ključne reči:** Nanostrukturna smeša; Mehanička aktivacija; Žarenje; Strukturna relaksacija; Specifična magnetizacija; Entalpija.

